

# Algebraic approach to a quarkyoniclike configuration and stable diquarks in dense matter

Aaron Park\* and Su Houg Lee<sup>†</sup>

*Department of Physics and Institute of Physics and Applied Physics, Yonsei University, Seoul 03722, Korea*



(Received 26 February 2022; accepted 6 June 2022; published 21 June 2022)

We study the color-spin interaction energy of a quark, a diquark and a baryon with their surrounding baryons and/or quark matter. This is accomplished by classifying all possible flavor and spin states of the resulting multi-quark configuration in both the flavor SU(2) and SU(3) symmetric cases. We find that while the baryon has the lowest interaction energy when there is only a single surrounding baryon, the quark has the lowest interaction energy when the surrounding has more than three baryons or becomes a quark gas. As the short range nucleon-nucleon interactions are dominated by the color-spin interactions, our finding suggests that the baryon modes near other baryons are suppressed due to larger repulsive energy compared to that of a quark and thus provides a quark model basis for the quarkyoniclike phase in dense matter. At the same time, when the internal interactions are taken into account, and the matter density is high so that the color-spin interaction becomes the dominant interaction, the diquark becomes the lowest energy configuration and will thus appear in both the dense baryonic and/or quark matter.

DOI: [10.1103/PhysRevD.105.114034](https://doi.org/10.1103/PhysRevD.105.114034)

## I. INTRODUCTION

Recent inputs from multimessenger astrophysics on a neutron star equation of state suggest that there is a sudden increase in pressure as one approaches the core of the neutron star [1]. Such behavior prompted the appearance of the quarkyonic matter type of equation of state (EOS) for the nuclear matter when the baryon density increases to several times that of the nuclear saturation density [2–11].

Recently, using the quark model with color-spin interaction, we have shown that the short distance repulsion between the quark and baryon is smaller than that between two baryons in the lowest energy channel, and that such ingredients naturally lead to a quarkyoniclike picture for the EOS when the baryon density reaches 4 to 5 times nuclear matter density [12]. The relevance of a color-spin interaction to describe the dynamics at short distance can be verified in several contexts. In a previous publication [13], we showed that the short distance part of the baryon-baryon interactions for various quantum numbers from the recent lattice calculation [14,15] can be well reproduced using a constituent quark model with color-spin interaction. The importance of color-spin interaction in nucleon-nucleon repulsion was observed earlier within the quark cluster model [16]. The mass splitting between hadrons with different spin orientations, such as the delta and the nucleon or the pseudoscalar and vector meson, are due to the color-

spin interaction [17]. Also studies on possible multi-quark configurations are based on the relative strength of the color-spin interaction of the multi-quark system compared to that of its lowest hadron threshold [18,19].

Therefore, when the quark density becomes large so that the baryons start to overlap, the color-spin interaction together with proper application of the Pauli principle should be the important dynamics that determines the properties of the dense matter. In this work, we will use the quark model with color-spin interaction to study the energy of a quark, diquarks and a baryon in the dense matter composed of baryons and in the quark matter. This is accomplished by classifying all possible flavor and spin states of the resulting multi-quark configurations in both the flavor SU(2) and SU(3) symmetric cases, and studying the color-spin interactions of these configurations.

We find that while the baryon has the lowest interaction energy when there is only a single surrounding baryon, the quark has the lowest interaction energy when the surrounding is composed of more than three baryons or becomes a quark gas. This is an improvement over our previous calculation [12] as all possible configurations are considered and the surroundings are generalized to study cases with more than one baryon and free quarks. Our finding implies that the baryon modes near other baryons are suppressed due to larger repulsive energy compared to that of a quark, which is a property when implemented into phenomenological EOSs composed of quarks and baryons leads to the appearance of quarkyoniclike phase in dense matter [4,5,12]. At the same time, when the internal

\* aaron.park@yonsei.ac.kr

† suhoung@yonsei.ac.kr

interactions are taken into account, and the matter density is high, similar to the quark density inside a baryon so that the color-spin interaction becomes the dominant interaction, the diquark becomes the lowest energy configuration and will thus appear in both the dense baryonic and/or quark matter.

It should be noted that our current result should be cast in the momentum space to provide a consistent comparison with the quarkyonic matter concept as described in [20]. One method to accomplish such a goal is to compare not only the short distance interaction but also the long distance interaction with the neighboring matter. A preliminary version of such a work was attempted in Ref. [12] using the uncertainty relation to convert the spatial interaction potential to the momentum space description of the excitation modes. We will leave a study along these lines as a future project.

The paper is organized as follows. In Sec. II, we introduce the color-spin interaction factor and explain how to calculate the interaction energy of a probe in nuclear matter. In Sec. III, we discuss how we classify the possible states of a multi-quark system and introduce the formula to calculate the average color-spin interaction factor. In Sec. IV, we discuss how we investigate the interaction energy of a probe when there is a noninteracting quark gas around it. In Sec. V, we discuss why we neglected the color-color interaction in this work by showing that the cross terms between a probe and nuclear matter cancel. In the last section, we summarize our results and discuss several prospects for future studies.

## II. COLOR-SPIN INTERACTION

In the flavor SU(3) symmetric case, the color-spin interaction factor is determined by the following form:

$$H_{CS} = - \sum_{i < j}^n \lambda_i^c \lambda_j^c \sigma_i \cdot \sigma_j \quad (1)$$

$$= n(n-10) + \frac{4}{3}S(S+1) + 4C_F + 2C_C, \quad (2)$$

$$4C_F = \frac{4}{3}(p_1^2 + p_2^2 + 3p_1 + 3p_2 + p_1 p_2), \quad (3)$$

where  $\lambda_i^c$  is the color SU(3) Gell-Mann matrices,  $C_F$  is the first kind of the Casimir operator of the flavor SU(3) and  $p_i$  is the number of columns containing  $i$  boxes in a column in the Young diagram. If there are no strange quarks, Eq. (2) reduces to the following formula:

$$H_{CS} = \frac{4}{3}n(n-6) + \frac{4}{3}S(S+1) + 4I(I+1) + 2C_C, \quad (4)$$

where  $I$  is the total isospin.

In the quark model for a hadron, there will be an extra spatial potential that depends on the distance between two particles multiplying the individual color-spin factor in Eq. (1) so that when calculating the total contribution of the relevant interactions to the hadron mass, the corresponding spatial expectation value has to be taken into account for each pair. On the other hand, assuming that all the quarks occupy similar spatial dimension and/or the quarks are uniformly distributed, the spatial parts will be universal for all quark pairs. Taking into account the additional factor that is inversely proportional to the quark masses of the pair, one finds that the delta-nucleon mass difference can be reproduced when  $C_B/m_u^2 \sim 18$  MeV [17]. This overall value should be multiplied to the color-spin factors in this work to estimate their approximate magnitude when the quark density is similar to that inside a nucleon. Therefore, to study the relative stability of different configurations, assuming that the density of quarks is uniform in the flavor symmetric limit, one can just compare the color-spin matrix elements given in Eq. (2).

Here, we calculate the color-spin factor experienced by a probe when the surroundings are  $n$  baryons, with  $n = 1, 2, 3$ , or a quark gas, all at a constant baryon density. The probe will be a quark, a diquark, or a baryon. As for the diquark, there are four kinds of diquarks that satisfy the Pauli principle. In this work, in order to focus on examining whether the diquark can exist as a stable state in high density nuclear matter we only consider the most attractive diquark where the flavor and spin are both antisymmetric. However, since various diquarks may appear as the density changes, the analysis of other types of diquarks will be included in the next study. The color of the quark and diquarks is in the triplet or antitriplet states, respectively, for which the free energy will be infinity in the confining phase where the surroundings are baryons. Hence, we also consider the color singlet three diquark state in flavor SU(3), whose quantum number is the same as the H dibaryon [21].

## III. FLAVOR, COLOR AND SPIN STATES OF A MULTIQUARK SYSTEM

Let us consider the multi-quark system consisting of  $n$  baryons with a probe. In this work, we assume that the orbital part of the wave function is totally symmetric and the surrounding baryons are in flavor octet states. Since a baryon is a color singlet, the color state of  $3n + n_p$  quarks, where  $n_p$  is the number of quark in the probe, should be in the color state of the probe. For example, if the probe is a baryon and  $n = 1$ , the color state of six quarks should be [2,2,2], which is a color singlet, and the flavor-spin coupling state should be the conjugate of the color singlet state to satisfy the Pauli exclusion principle. We can represent these states using Young diagrams as follows:

$$\text{Color : } \begin{array}{|c|c|} \hline \square & \square \\ \hline \square & \square \\ \hline \end{array}, \quad \text{Flavor} \otimes \text{Spin : } \begin{array}{|c|c|c|} \hline \square & \square & \square \\ \hline \square & \square & \square \\ \hline \end{array}$$

Then, we can decompose it into the flavor and the spin state as follows:

$$\begin{aligned} [3, 3]_{FS} = & [6]_F \otimes [3, 3]_S + [5, 1]_F \otimes [4, 2]_S + [4, 2]_F \otimes [5, 1]_S \\ & + [4, 2]_F \otimes [3, 3]_S + [4, 1, 1]_F \otimes [4, 2]_S \\ & + [3, 3]_F \otimes [6]_S + [3, 3]_F \otimes [4, 2]_S \\ & + [3, 2, 1]_F \otimes [5, 1]_S + [3, 2, 1]_F \otimes [4, 2]_S \\ & + [2, 2, 2]_F \otimes [3, 3]_S. \end{aligned} \quad (5)$$

Independently, we can determine the possible flavor states of a multi-quark system using the outer product:

Flavor states of 2-baryon:

$$\mathbf{8} \times \mathbf{8} = \mathbf{1} + \mathbf{8}_{(m=2)} + \mathbf{10} + \overline{\mathbf{10}} + \mathbf{27}. \quad (6)$$

Combining Eqs. (5) and (6), we can determine the possible flavor and spin states of six quarks. The allowed flavor and spin states for all cases that we consider are summarized in Table I.

Now, we investigate the relative magnitude of the interaction which a quark inside the probe sees from the surrounding  $n$  baryons using the following formula. A

TABLE I. List of possible flavor and spin states in flavor SU(3) symmetry. b, q and d represent a baryon, a quark and a diquark, respectively.

1b + 1b	$\mathbf{1}(S=0)$ , $\mathbf{8}(S=1)$ , $\mathbf{10}(S=1)$ , $\overline{\mathbf{10}}(S=1)$ , $\mathbf{27}(S=0)$
2b + 1b	$\mathbf{1}(S=\frac{3}{2})$ , $\mathbf{8}(S=\frac{1}{2}, \frac{3}{2})$ , $\mathbf{10}(S=\frac{3}{2})$ , $\overline{\mathbf{10}}(S=\frac{3}{2})$ , $\mathbf{27}(S=\frac{1}{2}, \frac{3}{2})$ , $\mathbf{35}(S=\frac{1}{2})$ , $\overline{\mathbf{35}}(S=\frac{1}{2})$ , $\mathbf{64}(S=\frac{3}{2})$
3b + 1b	$\mathbf{1}(S=0)$ , $\mathbf{8}(S=1, 2)$ , $\mathbf{10}(S=1)$ , $\overline{\mathbf{10}}(S=1)$ , $\mathbf{27}(S=0, 2)$ , $\overline{\mathbf{35}}(S=1)$ , $\mathbf{28}(S=0)$
1b + 1q	$\mathbf{3}(S=0, 1)$ , $\overline{\mathbf{6}}(S=0, 1)$ , $\mathbf{15}(S=0, 1)$
2b + 1q	$\mathbf{3}(S=\frac{1}{2}, \frac{3}{2})$ , $\overline{\mathbf{6}}(S=\frac{1}{2}, \frac{3}{2})$ , $\mathbf{15}(S=\frac{1}{2}, \frac{3}{2})$ , $\mathbf{15}'(S=\frac{1}{2}, \frac{3}{2})$ , $\mathbf{24}(S=\frac{1}{2}, \frac{3}{2})$ , $\mathbf{42}(S=\frac{1}{2}, \frac{3}{2})$
3b + 1q	$\mathbf{3}(S=0, 1, 2)$ , $\overline{\mathbf{6}}(S=0, 1, 2)$ , $\mathbf{15}(S=0, 1, 2)$ , $\mathbf{15}'(S=1)$ , $\overline{\mathbf{21}}(S=0)$ , $\overline{\mathbf{24}}(S=0, 1, 2)$ , $\mathbf{42}(S=0, 1, 2)$ , $\overline{\mathbf{60}}(S=1)$
1b + 1d	$\overline{\mathbf{3}}(S=\frac{1}{2})$ , $\mathbf{6}(S=\frac{1}{2})$ , $\overline{\mathbf{15}}(S=\frac{1}{2})$
2b + 1d	$\overline{\mathbf{3}}(S=0, 1)$ , $\mathbf{6}(S=1)$ , $\overline{\mathbf{15}}(S=0, 1)$ , $\mathbf{15}'(S=1)$ , $\overline{\mathbf{24}}(S=0, 1)$ , $\overline{\mathbf{42}}(S=0, 1)$
3b + 1d	$\overline{\mathbf{3}}(S=\frac{1}{2}, \frac{3}{2})$ , $\mathbf{6}(S=\frac{1}{2}, \frac{3}{2})$ , $\overline{\mathbf{15}}(S=\frac{1}{2}, \frac{3}{2})$ , $\mathbf{15}'(S=\frac{1}{2}, \frac{3}{2})$ , $\overline{\mathbf{24}}(S=\frac{1}{2}, \frac{3}{2})$ , $\overline{\mathbf{42}}(S=0, 1)$ , $\overline{\mathbf{48}}(S=\frac{1}{2})$
1b + 3d	$\mathbf{8}(S=\frac{1}{2})$
2b + 3d	$\mathbf{1}(S=0)$ , $\mathbf{8}(S=1)$ , $\overline{\mathbf{10}}(S=1)$ , $\mathbf{10}(S=1)$ , $\mathbf{27}(S=0)$
3b + 3d	$\mathbf{8}(S=\frac{1}{2})$ , $\overline{\mathbf{10}}(S=\frac{3}{2})$

similar formula was used previously by us to compare the nucleon repulsion with that of the lattice calculation [13]:

$$\Delta H_{CS}^{nb+p} = H_{CS}^{nb+p} - H_{CS}^{nb} - H_{CS}^p, \quad (7)$$

$$\Delta H_{CS}^{\text{avg}} = \frac{1}{n_p n \sum_{C,F,S} d_{CFS}} \sum_{C,F,S} d_{CFS} \Delta H_{CS}^{nb+p}, \quad (8)$$

$$d_{CFS} = d_C d_F d_S m_{FS}. \quad (9)$$

Here,  $nb$  and  $p$  in the superscripts represent  $n$  external baryons and the probe, respectively. The probe will be a baryon, a quark, a diquark or three correlated diquarks.  $n_p$  is the number of quarks in the probe. We will investigate cases with  $n = 1, 2, 3$ , and also consider the case where  $nb$  is replaced by a single quark so as to study the deconfined phase.  $d_C$ ,  $d_F$  and  $d_S$  are the dimensions of the color, flavor and spin states of  $3n + n_p$  quarks, respectively,  $m_{FS}$  is the multiplicity of the flavor and spin states, and the summation is taken for all possible states. Here, we divide it by  $n_p$  to normalize the result with respect to the single quark case. We also divide by  $n$  to keep the surrounding baryon at constant density for comparison at the same density.

#### IV. FREE QUARK GAS

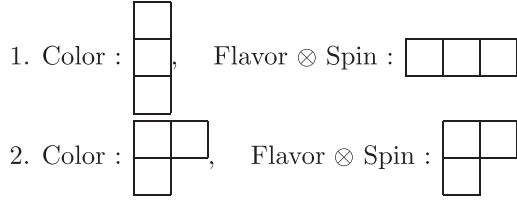
In this study, we increase the number of surrounding baryons correlated with each other to describe high density nuclear matter. However, when the density is very high, a phase in which the quarks are deconfined occurs, and at this stage, the quarks are no longer correlated with each other. Hence, in this section, we consider the case where the surrounding is a free quark gas. In such a case, we assume that the surrounding free quarks are not correlated with each other, but are correlated with the interacting object to satisfy the Pauli principle. Therefore, when a probe is a single quark, we only need to consider the average value of the color-spin interactions for all possible diquark configurations. There are four diquark states satisfying the Pauli principle. We represent it for the color SU( $N_C$ ) in Table II. If we compare it with the results for baryons and a

TABLE II. Classification of two quark interaction due to the Pauli exclusion principle. We denote the antisymmetric and symmetric state as A and S, respectively. The symbols inside the parentheses represent the multiplet state.

Flavor	$q_i q_j$			
	A	S	A	S
Color	A( $\overline{\mathbf{3}}$ )	A( $\overline{\mathbf{3}}$ )	S(6)	S(6)
Spin	A(1)	S(3)	S(3)	A(1)
$-\lambda_i \lambda_j \sigma_i \cdot \sigma_j$	$-6 - \frac{6}{N_C}$	$2 + \frac{2}{N_C}$	$-2 + \frac{2}{N_C}$	$6 - \frac{6}{N_C}$
$\lambda_i \lambda_j$	$-2 - \frac{2}{N_C}$	$-2 - \frac{2}{N_C}$	$2 - \frac{2}{N_C}$	$2 - \frac{2}{N_C}$

quark, then we should multiply it by 3 to ensure comparison at the same density.

For a diquark and a free quark, since  $\mathbf{3} \times \bar{\mathbf{3}} = \mathbf{1} + \mathbf{8}$ , there are two possible color states of three quarks, which will come with the flavor-spin configuration as below:



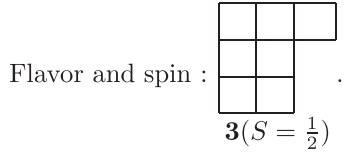
Considering both cases, we can calculate the average value of the color-spin interaction.

For the color-spin interaction between three correlated diquarks and a free quark, the color and flavor  $\otimes$  spin coupling state is as follows:



Flavor states of seven quarks:  $\mathbf{1} \times \mathbf{3} = \mathbf{3}$

Flavor states of 7 quarks :  $\mathbf{1} \times \mathbf{3} = \mathbf{3}$



The  $H_{CS}$  factors for this seven quarks state and the three correlated diquarks are  $-12$  and  $-24$ , respectively. In order to compare the result with the interaction factor when one baryon looks at one quark, we need to divide by 2, which corresponds to taking  $n_p = 6$ ,  $n = 1/3$  in Eq. (2).

For the color-spin interaction between a baryon and a quark, we can use the result in the previous discussions.

## V. COLOR-COLOR INTERACTION

The spin independent color-color type of interaction is typically responsible for the confining and Coulomb type of interactions. While such interactions are important at large separation between color states within a color singlet configuration, the interaction of a colored object with a color singlet configuration is small. In fact, it is zero if the color singlet configuration has no color polarizations: that is all quarks have the same spatial distribution. This is so because the color of the immersed object will be the same as the color of the multiquark configuration it makes with the surrounding color singlet baryons. Consider the following color-color interaction factor composed of  $n_p$  quarks from the probe and  $3n$  quarks from the  $n$  baryons:

$$\begin{aligned} \sum_{i<j}^{n_p+3n} \lambda_i^c \lambda_j^c &= \frac{1}{2} \left[ \left( \sum_i^{n_p+3n} \lambda_i^c \right)^2 - \sum_i^{n_p} (\lambda_i^c)^2 - \sum_i^{3n} (\lambda_i^c)^2 \right] \\ &= \frac{1}{2} \left[ \left( \sum_i^{n_p} \lambda_i^c \right)^2 - \sum_i^{n_p} (\lambda_i^c)^2 \right] - \frac{1}{2} \left[ \sum_i^{3n} (\lambda_i^c)^2 \right] \\ &= \sum_{i<j}^{n_p} \lambda_i^c \lambda_j^c + \sum_{i<j}^{3n} \lambda_i^c \lambda_j^c. \end{aligned} \quad (10)$$

In the second line, the first square bracket is the interaction within the probe while the second that between the color singlet baryons. That is, the contributions between the quarks in the probe and those in the color singlet configuration cancel out. The result is valid even for color  $SU(N_c)$  with any  $N_c$ .

## VI. RESULTS

As the color-color interactions cancel each other out, to understand the most stable structure at high density where the baryons start to overlap, we consider the color-spin interaction energy of a quark, a diquark or a baryon with the surrounding baryons. It should be noted that if the immersed object is an isolated colored object, it will require large energy to bring the isolated color charge to the position: this is why the thermal Wilson line is infinity in the confining phase. Therefore, we also consider the color singlet correlated three diquark state in flavor  $SU(3)$  case to search for the minimum energy configuration in the confining phase. However, when the quark density is large and color confining effects disappear or one is in the quark gas phase, the color of the immersed object can be neglected.

First, we represent  $\Delta H_{CS}^{\text{avg}}$  values between the probe and the surrounding for all cases in Table III. As can be seen in the table, when the surrounding is a single baryon, the baryon has the smallest interaction energy with the surrounding for both the flavor  $SU(2)$  and  $SU(3)$  cases. From the values in Table III, it can be seen that in the case of flavor  $SU(3)$ , the magnitude of the color-spin interaction of baryon is smaller than that of others by approximately 5 MeV per single quark if the density is similar to that inside a nucleon so that the previously estimated overall factor is used. However, when the surrounding becomes three baryon states or the free quark gas, a quark has the lowest interaction energy. In a series of work [4–7], Jeong *et al.* has shown that a phenomenological model involving quarks and baryons that leads to quarkyonic EOSs can be constructed when the short range baryon-baryon repulsion, through the excluded volume effect, is introduced. More recently, we have shown that in a realistic quark model, the short range quark-baryon repulsion is smaller than the baryon-baryon repulsion in the lowest energy channel, and that such difference leads to quarkyoniclike EOS. Here, we have shown that the quark-baryon repulsion is in general

TABLE III.  $\Delta H_{CS}^{\text{avg}}$  for different probes (column) in various surroundings (row). The upper and lower tables are for flavor SU(2) and SU(3), respectively.

$SU(2)_F$	1b	2b	3b	Free quarks	
Quark	8	8.533	6.133	4.364	
Diquark	8	8	8	8	
Baryon (octet)	7.111	7.111	7.111	8	
$SU(3)_F$	1b	2b	3b	Free quarks	
Quark		6	6.446	4.644	2.823
Diquark		6	6.176	5.551	6.3
Three correlated diquarks		6	6	6	6
Baryon (octet)		5.714	5.78	4.944	6

smaller than the baryon-baryon repulsion at high baryon density or free quark gas. Our results show that the probe that feels the lowest color-spin interaction that dominates the repulsion at short distance is quark rather than baryon, which provides a theoretical justification for the quarkyoniclike phase.

Second, to determine which probe has lower energy in dense matter, one has to consider the internal color-spin factor of the immersed object. The octet baryon and the diquark both have color-spin factors of  $-8$ . The additional kinetic energy within the probe typically cancels the color-color interaction strength rendering the color-spin interaction to be the only relevant interaction strength within the probe [22,23]. Table IV shows the results after considering these internal color-spin factors. It can be seen that the lowest energy configuration in both the baryon matter and quark matter is the diquark for flavor SU(2) and the color singlet three correlated diquarks for flavor SU(3). Therefore, considering confinement, the color singlet three correlated diquarks is the most stable configuration in dense baryonic matter, when the density becomes similar to the quark density within the baryon so that only the color-spin interaction becomes relevant. Such configurations will appear in dense baryonic matter. Hence, while H dibaryons do not seem to exist in the vacuum [24], similar configurations will appear in dense baryonic matter. When deconfinement takes place, considering the additional strange quark mass in the color singlet three diquarks, flavor SU(2) diquarks will also appear contributing as an important configuration in dense matter: hence, a diquark matter.

TABLE IV. Same as Table III after internal interactions within the probes are considered.

$SU(2)_F$	1b	2b	3b	Free quarks	
Quark	8	8.533	6.133	4.364	
Diquark	4	4	4	4	
Baryon (octet)	4.444	4.444	4.444	5.333	
$SU(3)_F$	1b	2b	3b	Free quarks	
Quark		6	6.446	4.644	2.823
Diquark		2	2.176	1.551	2.3
Three correlated diquarks		2	2	2	2
Baryon (octet)		3.048	3.113	2.277	3.333

Additionally, if one can show that the interaction between correlated diquarks is relatively more attractive than the corresponding values involving baryons or quarks, then the so-called diquarkyonic matter consisting of diquarks and baryons or diquark condensation may emerge.

There are a few things to remark for the next study. In this work, we only consider the most attractive diquark state. However, since the interaction of the other diquarks with the surrounding matter might be more attractive than that for the most attractive diquark, we should investigate the possible occurrence of such additional diquarks. Additionally, after the study of a dual chiral density wave [25], which is one of the inhomogeneous chiral phases, it has been investigated that quarkyonic matter could be spatially inhomogeneous due to the appearance of chiral density waves [11,26,27]. Inhomogeneous phases were also studied based on the Nambu–Jona-Lasinio model and the Gross-Neveu model [28,29]. Although we only consider spatially symmetric wave function in this work, analysis on a spatially inhomogeneous condensate needs to be investigated.

## ACKNOWLEDGMENTS

This work was supported by Samsung Science and Technology Foundation under Project No. SSTF-BA1901-04. The work of A.P. was supported by the Korea National Research Foundation under the Grant No. 2021R1I1A1A01043019. The authors would like to thank Kiesang Jeong and Hyungjoo Kim for useful discussions.

- [1] T. Kojo, G. Baym, and T. Hatsuda, [arXiv:2111.11919](#).  
 [2] L. McLerran and R. D. Pisarski, *Nucl. Phys.* **A796**, 83 (2007).  
 [3] L. McLerran and S. Reddy, *Phys. Rev. Lett.* **122**, 122701 (2019).

- [4] K. S. Jeong, L. McLerran, and S. Sen, *Phys. Rev. C* **101**, 035201 (2020).  
 [5] S. Sen and N. C. Warrington, *Nucl. Phys.* **A1006**, 122059 (2021).

- [6] D. C. Duarte, S. Hernandez-Ortiz, and K. S. Jeong, *Phys. Rev. C* **102**, 025203 (2020).
- [7] D. C. Duarte, S. Hernandez-Ortiz, and K. S. Jeong, *Phys. Rev. C* **102**, 065202 (2020).
- [8] S. Sen and L. Sivertsen, *Astrophys. J.* **915**, 109 (2021).
- [9] T. Zhao and J. M. Lattimer, *Phys. Rev. D* **102**, 023021 (2020).
- [10] J. Margueron, H. Hansen, P. Proust, and G. Chanfray, *Phys. Rev. C* **104**, 055803 (2021).
- [11] T. Kojo, Y. Hidaka, L. McLerran, and R. D. Pisarski, *Nucl. Phys.* **A843**, 37 (2010).
- [12] A. Park, K. S. Jeong, and S. H. Lee, *Phys. Rev. D* **104**, 094024 (2021).
- [13] A. Park, S. H. Lee, T. Inoue, and T. Hatsuda, *Eur. Phys. J. A* **56**, 93 (2020).
- [14] N. Ishii, S. Aoki, and T. Hatsuda, *Phys. Rev. Lett.* **99**, 022001 (2007).
- [15] T. Inoue, N. Ishii, S. Aoki, T. Doi, T. Hatsuda, Y. Ikeda, K. Murano, H. Nemura, and K. Sasaki (HAL QCD Collaboration), *Prog. Theor. Phys.* **124**, 591 (2010).
- [16] M. Oka, K. Shimizu, and K. Yazaki, *Prog. Theor. Phys. Suppl.* **137**, 1 (2000).
- [17] S. H. Lee, S. Yasui, W. Liu, and C. M. Ko, *Eur. Phys. J. C* **54**, 259 (2008).
- [18] A. Park, W. Park, and S. H. Lee, *Phys. Rev. D* **96**, 034029 (2017).
- [19] S. Noh, W. Park, and S. H. Lee, *Phys. Rev. D* **103**, 114009 (2021).
- [20] K. Fukushima, T. Kojo, and W. Weise, *Phys. Rev. D* **102**, 096017 (2020).
- [21] R. L. Jaffe, *Phys. Rev. Lett.* **38**, 195 (1977).
- [22] W. Park, S. Noh, and S. H. Lee, *Nucl. Phys.* **A983**, 1 (2019).
- [23] M. Karliner and J. L. Rosner, *Phys. Rev. Lett.* **119**, 202001 (2017).
- [24] W. Park, A. Park, and S. H. Lee, *Phys. Rev. D* **93**, 074007 (2016).
- [25] E. Nakano and T. Tatsumi, *Phys. Rev. D* **71**, 114006 (2005).
- [26] T. Kojo, Y. Hidaka, K. Fukushima, L. D. McLerran, and R. D. Pisarski, *Nucl. Phys.* **A875**, 94 (2012).
- [27] I. E. Frolov, V. C. Zhukovsky, and K. G. Klimenko, *Phys. Rev. D* **82**, 076002 (2010).
- [28] D. Nickel, *Phys. Rev. Lett.* **103**, 072301 (2009).
- [29] D. Nickel, *Phys. Rev. D* **80**, 074025 (2009).